SMAR 2017 – Fourth Conference on Smart Monitoring,
Assessment and Rehabilitation of Civil Structures

SMAR 2017

Development, testing, and FEA of a SMA/CFRP patch for repair of cracked metallic structures

Mina Dawood[1], Botong Zheng[2], and Mossab El-Tahan[3]

[1] University of Houston, Houston, USA
[2] University of Houston, Houston, USA
[3] DAR Group, Cairo, Egypt

ABSTRACT: This paper summarizes the details of an experimental and numerical research program that was conducted to develop a new type of shape memory alloy (SMA)/carbon fiber reinforced polymer (CFRP) patching system for repair of cracked and crack-sensitive metallic structural components. The system development included a study of the bond between SMA wires and CFRP tabs, evaluation of the maximum prestressing force that can be generated by the SMA wires, and assessment of the loss of prestressing force due to fatigue. The effectiveness of the system was validated experimentally through a series of 27 fatigue tests of single-edge notched steel coupons subjected to tension-tension fatigue loading. Debonding of the patches from the steel surface due to crack propagation was monitored using a digital image correlation- (DIC) based measurement system. A numerical modeling approach was developed to predict the fatigue life and generate the crack growth curves of the repaired elements. The results indicated that the SMA/CFRP patching system can effectively increase the expected fatigue life of crack-sensitive components by up to 26 times. The findings suggest that the SMA/CFRP patch is a promising new technology for retrofitting cracked and crack-sensitive metallic structural components.

1 INTRODUCTION

Externally bonded fiber reinforced polymer (FRP) composites have been used to rehabilitate fatigue damaged or fatigue sensitive structures (Jones and Civjan, 2003; Tavakkolizadeh and Saadamanesh, 2003; Liu et al., 2009). Recently, prestressed FRP patches were found to be more effective for fatigue life enhancement than non-prestressed patches (Täljsten et al., 2009; Ghafoori et al., 2012). However, the conventional methods of achieving an appropriate level of prestressing not only require heavy equipment, but also are designed for applying global prestressing rather than locally strengthening cracks. Consequently, there is a need to identify a technique to practically apply prestressing forces to the FRP to effectively improve the life of fatigue sensitive details. Prestrained shape memory alloy (SMA) materials exhibit a unique thermo-mechanical response through which, when they are heated, they return to their un-prestrained geometry. By restraining this transformation, prestrained SMAs can be used to apply recovery forces, or prestressing forces, to structural elements. This property of SMA materials has been exploited to develop composites that are able to actively tune their mechanical response (Epps and Chandra, 1997; Song et al., 2000; Bollas *et al*., 2007). The effectiveness of the SMA/CFRP composite relies on the effective bond between the two materials. Research has been conducted to investigate the debonding failure mechanism (Lau et al., 2002) and develop a model to predict the debonding stress and critical bond length (Poon et al., 2005; Payandeh et al., 2012). Ternary nickel-titanium- niobium (NiTiNb) SMA have been developed to ensure a wide thermal hysteresis with high activation temperatures (~160ºC) and low reverse transformation temperatures (~ -50ºC), making them well suited for applications that require sustained recovery forces at or near room temperature (Melton et al 1989, Shin and Andrawes 2010).

2 DEVELOPMENT OF SMA/CFRP PATCHING SYSTEM

A novel SMA and carbon FRP (CFRP) composite was developed to rehabilitate metallic elements with fatigue sensitive details. SMA wires were employed to replace the conventional prestressing method to apply compressive stresses to the steel substrate. CFRP overlay was designed to bridge the crack path and protect the underlying SMA wires. The effectiveness of the system relies on the bond between SMA wires and CFRP patches, which was investigated through pullout tests. Further, the composite patch was tested under monotonic and fatigue loading to evaluate the prestress level that can be achieved and the stability of the prestress level during fatigue loading.

2.1 Concept description

The SMA/CFRP patching system consists of an inner layer of SMA wires and an outer layer of CFRP overlay, as illustrated in Figure 1(a). SMA wires were sandwiched into a two-layer CFRP matrix, which were made using high modulus carbon fibers and Araldite 420 saturating resin. The wires had a spacing equal to the wire diameter and an embedment length of 76 mm at each end. Forty-six wires were used in each patch. Upon thermal activation, the inner layer generates a recovery stress to induce compressive stresses around the fatigue sensitive detail or crack tip in the metallic substrate. Figure 1(b) shows the temperature-recovery stress relationship of three SMA wires. Upon heating the wire to 160˚C, the generated recovery stress was 400 MPa. When the wire was cooled to room temperature, the recovery stress remained constant. According to the manufacturer (Intrinsic Devices, San Francisco, California), this level of recovery stress should be sustainable to temperatures as low as -50ºC. Figure 1(c) shows the relationship between the compressive stress in the steel substrate and the temperature of the SMA wires during the thermal activation. The temperature was monitored using two thermocouples, one on each side of the steel plate. The resulting compressive stress in the steel after cooling to room temperature was approximately 17 MPa after activating the SMA patches on both sides of the steel plate. The target stress in the SMA wires after activation was 235 MPa. The stiffness of the SMA wires was 0.2% that of the steel plate. Therefore, the stresses induced in the SMA wires due to cyclic loads were negligible compared to the activation stress. No out-of-plane bending deformation was observed during the activation. This compressive stress reduces the maximum stress intensity factor (SIF) at the crack tip at a given load and hence allows the crack to grow longer before reaching the critical crack length.

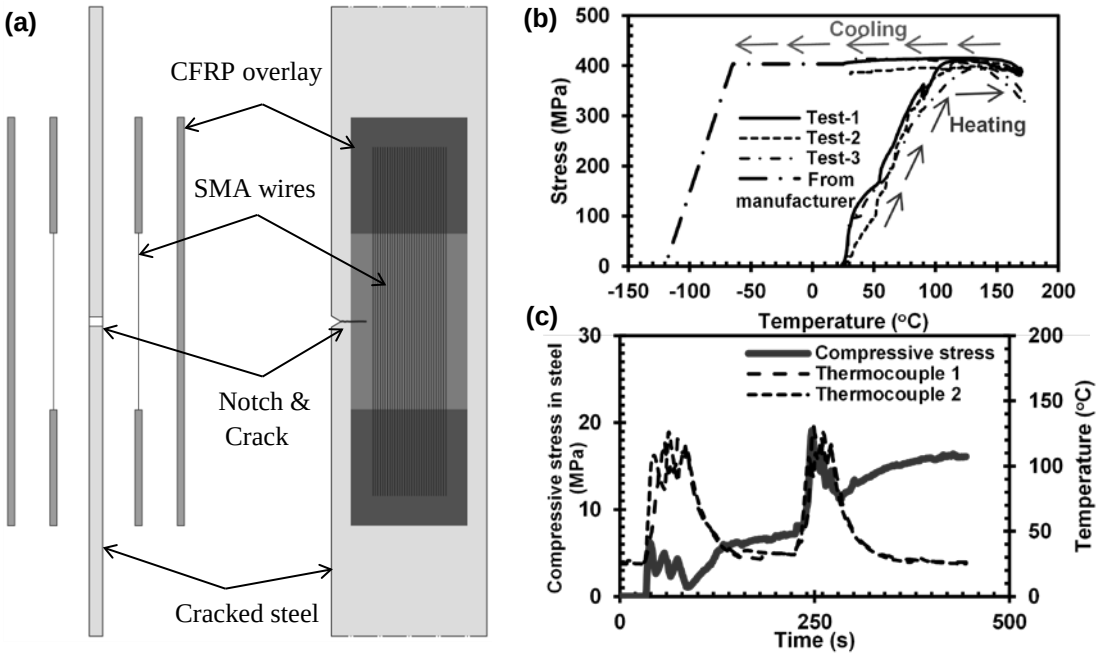

Figure 1. (a) Schematic of the SMA/CFRP patching system, (b) thermomechanical behavior of the SMA material, (c) compressive stress in the steel due to activation of the SMA wires

2.2 Bond between SMA and CFRP

Nine pullout tests were conducted to investigate the bond behavior of NiTiNb SMA wires to CFRP. Figure 2(a) shows the coupon and test setup. Extensometers were used to monitor the strain and interfacial slip while the DIC system was used to identify the onset and propagation of debonding. Figure 2(b) shows the results of the longitudinal strain contours obtained from the DIC system, and the relationship between load and relative displacement between SMA and CFRP (recorded by the 12.7 mm extensometer). Each contour image corresponds to the square markers on the load-displacement curve sequentially. A localized strain concentration is seen in the first contour image. As load increases, the size and intensity of the concentration increases until the load reached 200 N. Thereafter, the strain concentration shifted towards the other end of the CFRP patch indicating propagation of the debonding. The onset load of the debonding is 200 N while the complete debonding occurred at a load of 250 N. Similar trends and results were observed for the rest of the coupons.

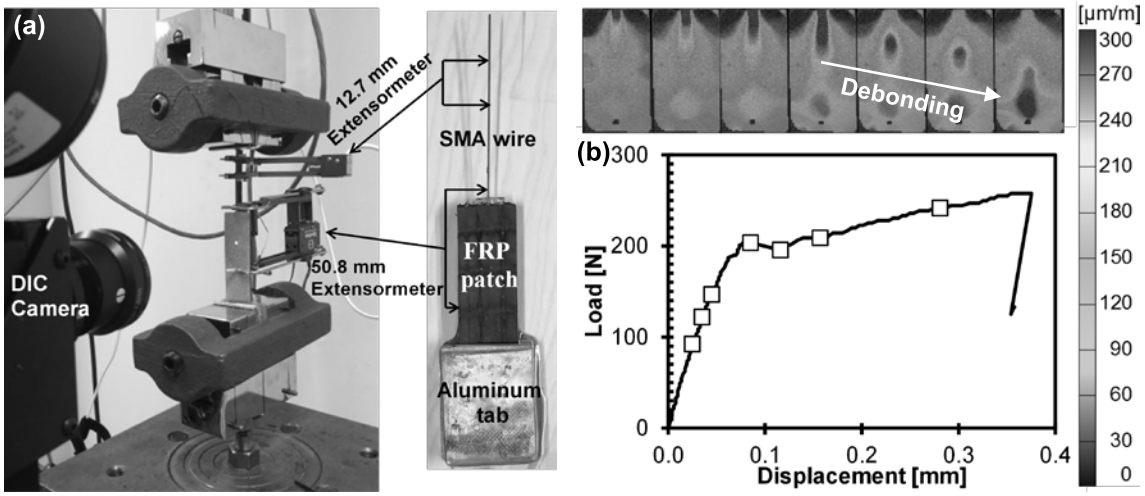

Figure 2. (a) Pullout coupon and test setup; (b) load-slip curve and the corresponding DIC data

2.3 Monotonic and fatigue behavior of SMA/CFRP patch

Two SMA/CFRP patches were tested to evaluate the recovery stress that can be achieved. A total of 14 SMA/CFRP patches were tested to evaluate the stability of the recovery stress under fatigue loading considering the influence of the recovery stress level and applied stress range. Figure 3 shows the schematic of the test coupon containing ten 0.77 mm diameter NiTiNb SMA wires with spacing of 0.89 mm. A recovery force of 1750 N (370 MPa recovery stress in the SMA wires) was measured for both of the coupons after the SMA wires were activated. This suggests that the recovery force was effectively proportional to the number of wires in the patch for the configuration tested. After the activation, both coupons were tension loaded up to failure. The average capacity of the coupons was 3300 N.

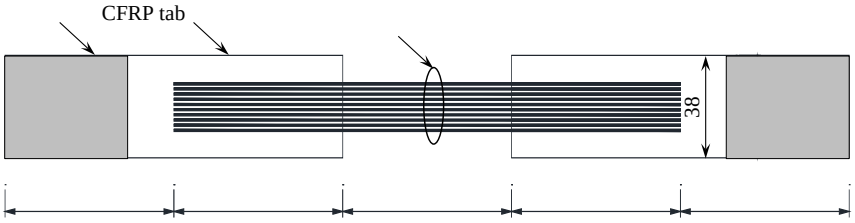

Figure 3 SMA/CFRP test coupon containing 10 SMA wires

For the fatigue testing, the coupons were divided into three groups based on the recovery stress level and applied stress range. The stress inducing the onset of the debonding between SMA and CFRP was identified as 400 MPa. In Group I and II, the recovery stress level of 250 MPa was selected to prevent debonding upon activation. In Group III, the SMA wires were fully activated to 400 MPa which could induce the onset of debonding. The tested stress ranges of the three groups are shown in Figure 4(a). The SMA wires in Group I experienced maximum stresses that were lower than the debonding onset stress; those in Group II and III experienced higher stress than the debonding onset stress. Figure 4(b) shows the normalized recovery stress level against the number of fatigue cycles. It is seen that Group I maintained 80% of the recovery stress after 2 million cycles. Group II and III, however, completely lost the recovery stress after 0.03 and 0.1 million cycles, respectively. This suggests that in order for the system to maintain the recovery stress level, the maximum stress of the SMA wires has to be less than the debonding onset stress.

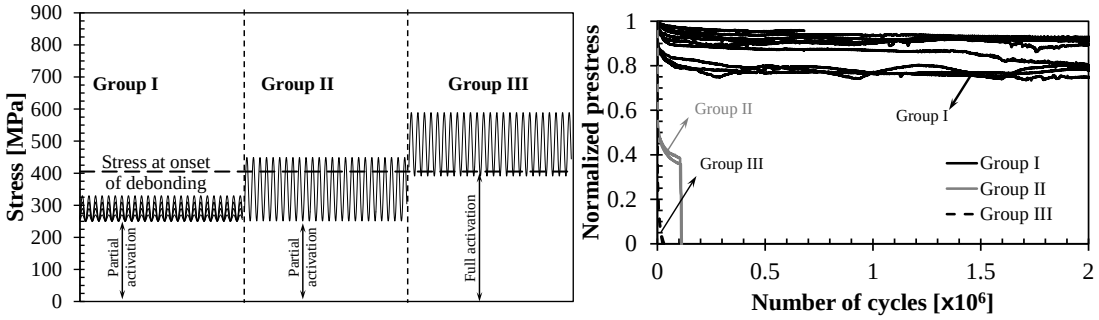

Figure 4. (a) Stress ranges for three groups, (b) recovery stress level and number of load cycles

3 FATIGUE STRENGTHENING OF STEEL ELEMENT USING THE SMA/CFRP PATCH

The effectiveness of the developed SMA/CFRP patch for repair of fatigue-sensitive steel elements was evaluated through fatigue testing of twenty-seven single edge-notched steel coupons. Four groups of coupons were prepared and tested under high-cycle tension-tension fatigue loading: (i) 'Steel' group, un-strengthened, plain steel control coupons, (ii) 'CFRP' group, coupons patched with CFRP only, (iii) 'SMA' group, coupons patched with activated SMA wires only (without the FRP overlay), and (iv) 'SMA/CFRP' group, coupons patched with the SMA/CFRP composite patches. Three stress ranges, 217 MPa, 155MPa and 93 MPa were considered for Steel and CFRP groups. The SMA group was tested under 155 MPa stress range. The SMA/CFRP group was tested under 217 and 155 MPa stress ranges. Three repetitions were tested for each configuration.

Figure 5(a) shows the test setup. The crack front was traced using the beach marking technique (Yu et al. 2013). The surface of the CFRP overlay was monitored using DIC system to investigate the debonding during fatigue loading. Figure 5(b) shows the surface longitudinal strain contours that indicate the strain concentration along the fatigue crack at different stages. The figure also indicates the number of loading cycles and the simultaneous crack length at which each of the images was recorded. No strain concentration was observed in the first contour at 81,000 fatigue cycles since the crack had not propagated underneath the CFRP overlay. After 170,250 cycles the strain concentration around the crack indicates the presence of a debonded region that extended from the crack tip to the edge of the CFRP patch towards the edge of the plate where the crack mouth was located. The shape of the debonded region was initially semi-elliptical but evolved into an approximately triangular shape as the crack propagated. Similar patterns and trends of the strain concentrations and the corresponding crack lengths were observed for the other coupons. The size and shape of the debonded region of the patches was determined from the DIC measurements by considering this strain gradient. Since the strain gradient is proportional to the adhesive shear stress. The experimental observations in this research suggest that the fatigue loading does not impact the debonding directly. Rather, fatigue loading causes propagation of the crack in the steel and the increase of the crack length drives the propagation of the debonded region.

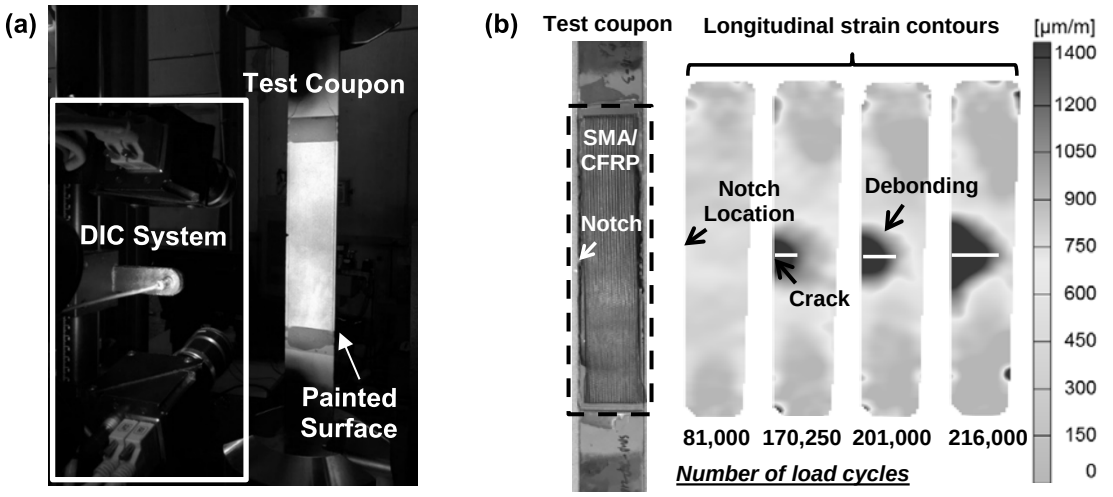

Figure 5. (a) Test setup; (b) surface strain contours of CFRP overlay at different stages

Figure 6(a) plots the measured fatigue lives of the tested coupons against the stress range. The fatigue lives for AASHTO fatigue categories B', C, D and E (AASHTO, 2012) are also indicated in the figure for comparison. The Steel group had fatigue lives that fell below those of AASHTO fatigue category E. Installation of the CFRP patch increased the average fatigue life of the coupon to 3.0 and 8.7 times that of the control coupons at stress ranges of 217 MPa and 155 MPa, respectively. CFRP patched specimens that were tested at a stress range of 93 MPa exhibited fatigue lives of more than 2 million cycles without any appreciable crack propagation.

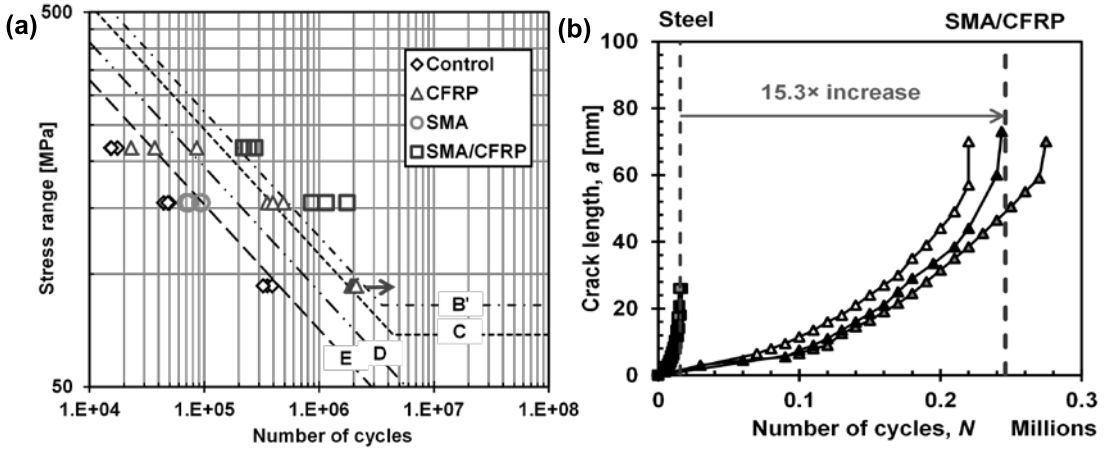

Figure 6. (a) S-N chart for all of the tested coupons; (b) crack growth curves of Steel and SMA/CFRP at 217 MPa stress range

The coupons that were patched with prestressed SMA wires exhibited an average fatigue life that was 1.7 times that of the control group at a stress range of 155 MPa. In comparison, the coupons that were patched with SMA/CFRP patches exhibited average fatigue lives that were 15.3 times and 26.4 times those of the unpatched coupons for stress ranges of 217 MPa and 155 MPa, respectively. Comparison of the strengthening effect of the SMA/CFRP group with the SMA and CFRP groups indicates that there is a synergistic effect between the SMA wires and the CFRP overlay. Figure 6(b) compares the crack growth curves between the SMA/CFRP and Steel groups of coupons that were tested at 217 MPa stress range. The SMA/CFRP patches increased the average fatigue lives by 15.3 times. It is seen that not only the crack growth rate

(the slope of the curve) of the SMA/CFRP group is substantially decreased, but also the crack length at which the coupons fractured was increased from 26 mm to 75 mm.

4 NUMERICAL MODELING

A numerical framework was established to simulate the fatigue crack growth (FCG) of the patched steel elements. The interfacial debonding was considered through incorporating a finite element (FE) model that is able to predict the debonded region and calculate the SIF. Figure 7(a) shows the model that predicts the debonded region at a given crack length. The Steel/CFRP interface was simulated using a cohesive zone governed by a bilinear traction-separation behavior as indicated in the figure. Figure 7(b) compares the debonded region of a SMA/CFRP group of coupons with crack length of 70 mm that was predicted by the numerical model (left image) and calculated from the DIC data (right image). The left image indicates the debonded region through the damage parameter, λ, of which a value equal to 1 indicates complete debonding at that location. The right image shows the longitudinal strain gradient distribution on the surface of the CFRP. The region that is bounded by the high shear stress and has less than 0.002 μm/m/m strain gradient, is considered as debonded. The close correlation between the numerically and experimentally obtained debonded regions validates the debonding prediction.

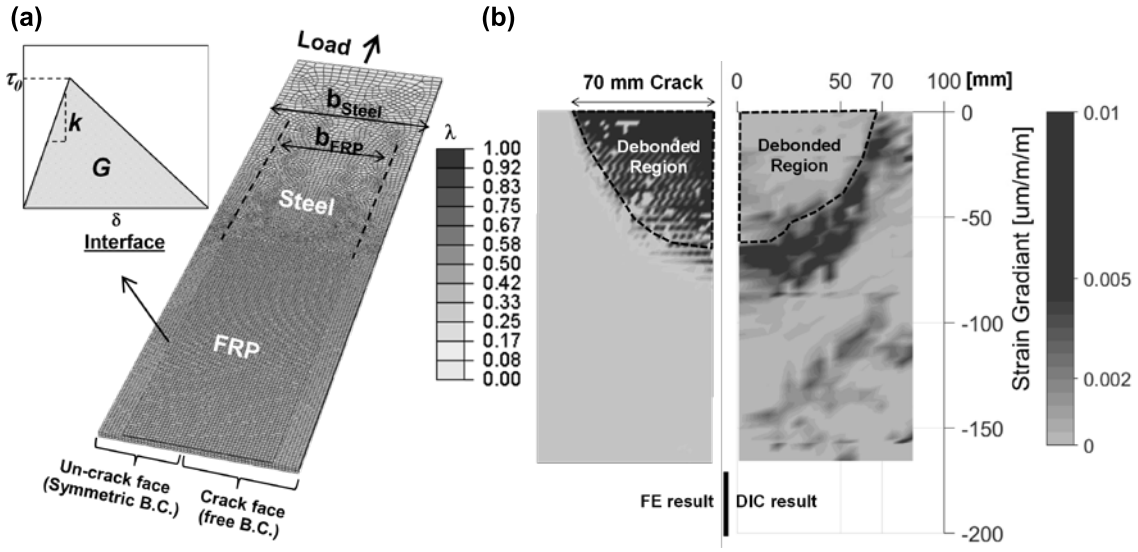

Figure 7. (a) FE model to predict the debonding (b) comparison of the debonded region from FE prediction and DIC data

The predicted debonded regions corresponding to different crack lengths were then used to calculate the SIF for different crack lengths in a separate FE model as shown in Figure 8(a). The stress singularity at the crack tip was represented using classical 3-D, wedge-shaped crack tip elements, which are collapsed 20-node elements with edge nodes shifted to the 1/4 point along the edges. Figure 8(b) shows the calculated maximum SIF at different crack lengths for CFRP and SMA/CFRP groups. It is seen that SMA/CFRP coupons exhibited much lower maximum SIF values than those in the CFRP group. The fracture toughness of the steel was taken conservatively as 2000 MPa·mm$^{1/2}$ in this research.

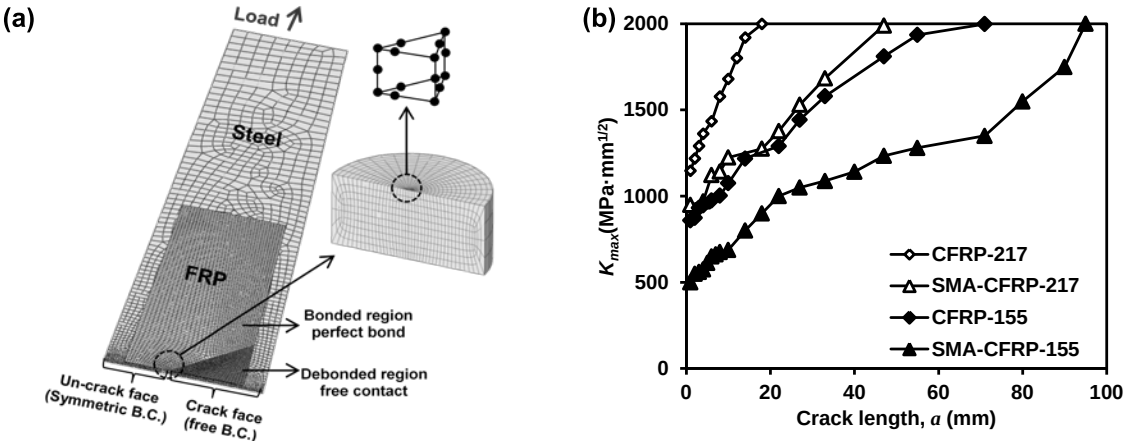

Figure 8 (a) FE model to calculate SIF; (b) maximum SIF of CFRP and SMA/CFRP groups

Subsequently, crack growth rates were calculated at discrete crack lengths a_i (i = 0 to n). The corresponding number of fatigue cycles, N_i, that elapsed as the crack propagated from a_0 to a_i was calculated based on the discrete form of the crack growth model, illustrated in Figure 9(a). Figure 9(b) shows the comparison of the FCG curves between the numerical and experimental results of the SMA/CFRP group of coupons that were tested at a stress range of 217 MPa. The close correlation between the measured and predicted FCG curves validates the numerical framework.

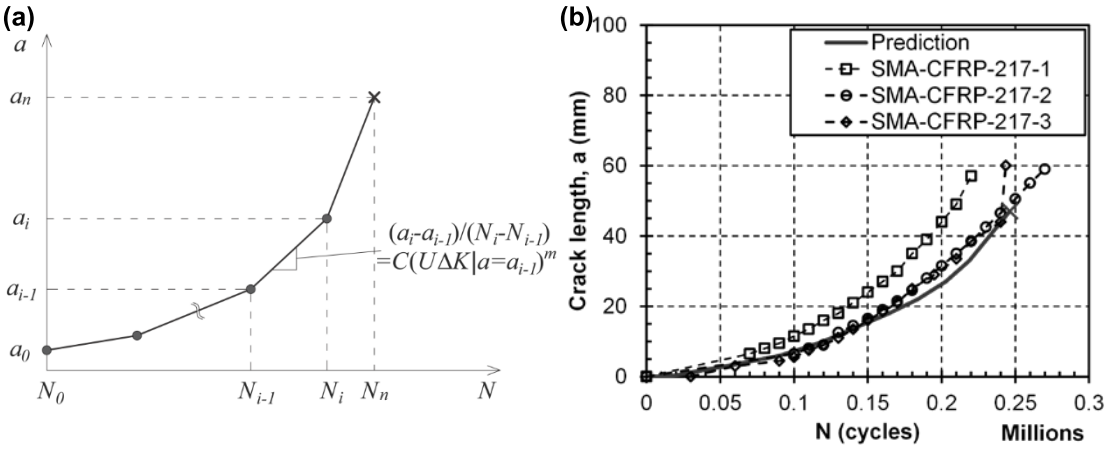

Figure 9. (a) Illustration of crack growth analysis; (b) predicted and tested crack growth curves

5 SUMMARY AND CONCLUSIONS

Prestrained SMA wires were embedded into CFRP patches to develop a novel composite that can be used to improve the fatigue resistance of metallic elements. The composite patch containing 10 SMA wires was able to generate 1750 N recovery force upon heating up to 160ºC. The composite that was bonded to the surface of a steel plate induced 17 MPa compressive stress in the steel substrate upon thermal activation. Fatigue testing of the composite coupon indicated stable prestress level could be maintained as long as the maximum stress in the SMA wires is less than the stress at the onset of debonding. Fatigue testing of single edge-notched steel plates that were reinforced with the SMA/CFRP composites indicated 15 and 26 times fatigue life improvement compared with un-strengthened coupons at 155 and 217 MPa stress ranges, respectively. A numerical framework considering the interfacial

debonding was developed to simulate the FCG of the SMA/CFRP patched steel element. The close agreement between the predicted and experimental FCG curves validates the framework. The findings collectively suggest that the proposed SMA/CFRP patches are a promising technique to repair fatigue sensitive details in metallic structures.

6 REFERENCES

AASHTO (American Association of State Highway and Transportation Officials). (2012). "LRFD bridge design specifications," Washington, DC.

Bollas, D., Pappas, P., Parthenios, J., & Galiotis, C. (2007). "Stress generation by shape memory alloy wires embedded in polymer composites." Acta Materialia, 55(16), 5489–5499.

Lau, K., Chan, A., Shi, S., and Zhou, L. (2002). Debond induced by strain recovery of an embedded NiTi wire at a NiTi/epoxy interface: micro-scale observation. Materials and Design, 23(3), 265-270.

Epps, J., and Chandra, R. (1997). Shape memory alloy actuation for active tuning of composite beams. Smart Materials and Structures, 6(3), 251-264.

Ghafoori, E., Schumacher, a., & Motavalli, M. (2012). "Fatigue behavior of notched steel beams reinforced with bonded CFRP plates: Determination of prestressing level for crack arrest." Engineering Structures, 45, 270–283.

Jones, S., & Civjan, S. (2003). "Application of fiber reinforced polymer overlays to extend steel fatigue life." Journal of Composites for Construction, (November), 331–338.

Liu, H., Al-Mahaidi, R., & Zhao, X.-L. (2009). "Experimental study of fatigue crack growth behaviour in adhesively reinforced steel structures." Composite Structures, 90(1), 12–20.

Melton, K., Proft, J., and Duerig, T. (1989). Wide hysteresis shape memory alloys based on the NiTINb system. Materials research society international symposium proceedings.

Payandeh, Y., Meraghni, F., Patoor, E., and Eberhardt, A. (2012). Study of the martensitic transformation in NiTi-epoxy smart composite and its effect on the overall behavior. Materials and Design, 39, 104-110.

Poon, C., Zhou, L., Jin, W., and Shi, S. (2005). Interfacial debond of shape memory alloy composites. Smart Materials and Structures, 14(4), N29-N37.

Shin, M., and Andrawes, B. (2010). Experimental investigation of actively confined concrete using shape memory alloys. Engineering Structures, 32(3), 656-664.

Song, G., Kelly, B., and Agrawal, B. (2000a). Active position control of a shape memory alloy wire actuated composite beam. Smart Materials and Structures, 9(5), 711-716.

Täljsten, B., Hansen, C. S., & Schmidt, J. W. (2009). "Strengthening of old metallic structures in fatigue with prestressed and non-prestressed CFRP laminates." Construction and Building Materials, 23(4), 1665–1677.

Tavakkolizadeh, M., & Saadatmanesh, H. (2003). "Fatigue Strength of Steel Girders Strengthened with Carbon Fiber Reinforced Polymer Patch." Journal of Structural Engineering, 129(2), 186–196.

Yu, Q., Chen, T., Gu, X., Zhao, X., and Xiao, Z. (2013). "Fatigue behavior of CFRP strengthened steel plates with different degrees of damage." Thin Walled Structures, 69, 10–17.